

Triggering wave-domain heat conduction in graphene



Wen-Jun Yao, Bing-Yang Cao*

Key Laboratory for Thermal Science and Power Engineering of Ministry of Education, Department of Engineering Mechanics, Tsinghua University, Beijing 100084, PR China

ARTICLE INFO

Article history:

Received 16 March 2016
 Received in revised form 12 April 2016
 Accepted 16 April 2016
 Available online 19 April 2016
 Communicated by R. Wu

Keywords:

Non-Fourier heat conduction
 Graphene
 Mechanical wave
 Molecular dynamics simulation

ABSTRACT

Using non-equilibrium molecular dynamics simulations, we systematically investigate the non-Fourier heat conduction in graphene under steady high heat flux. The results show that if two triggering factors, i.e. steady high heat flux and tensile stress, are satisfied simultaneously, a low-frequency mechanical wave and corresponding wave-like energy profile can be observed, which are distinctly different from ripples and linear temperature profile of the normal Fourier heat conduction. This mechanical wave provides an additional channel of heat transport and renders graphene more conductive without changing its pristine thermal conductivity. What's more, as the heat flux or original bond length increases, its frequency increases and energy transported by this mechanical wave is also on the rise. Further analyses show that such anomalous phenomenon is not arising from the high-energy or high-frequency pulses and also not artifacts of the velocity-exchange method. It is a dissipative structure, a new order state far from thermodynamic equilibrium, and the corresponding nonlinear relationship between the gradient of the wave-like kinetic temperature and the heat flux enables more efficient heat transport in graphene.

© 2016 Elsevier B.V. All rights reserved.

1. Introduction

The combination of high-efficiency heat dissipation and low-handling thermal management makes graphene a promising candidate material for energy, electronics, and optical applications [1–4]. In the past decade, large amount of studies have been dedicated to heat transport in graphene [1,3–20], considerable part of which deals with its reducible thermal conductivity under low heat fluxes, where phonons are blocked or scattered by defects [11–14], dopants [11,12,15,16], strain [17,18] and so on [19,20]. These studies show a tunable thermal conductivity of over 25 times and a high thermoelectric figure of merit ZT of 2~3 [12,14,19], making graphene possible for thermoelectrics. But for high power or high frequency applications, the heat dissipation, manipulation or even enhancement of thermal conductivity of graphene at high heat fluxes is still a challenge.

Earlier studies demonstrated that in low dimensional materials, the non-Fourier heat conduction is easy to be activated by instantaneous high heat fluxes [21–23]. For example, if imposing a local heating with a duration of 1 ps into graphene, a thermal wave, symbol of non-Fourier heat conduction, would be observed [23]. Likewise, non-Fourier heat conduction could also occur at steady high heat fluxes. Recently, Zhang et al. [24] first reported that as

the steady high heat flux exceeds a critical value, a low-frequency transverse acoustic wave will be excited in single-walled carbon nanotubes (CNT), which results in an anomalous temperature profile and transports energy effectively. Similar mechanical waves were also observed in graphene nanoribbons and hybrid GE/SE monolayers under steady high heat flux conditions [25,26]. This non-Fourier heat conduction mechanism suggests a totally fresh idea of solving heat dissipation. But this is only the beginning. How to trigger this wave-domain transport mode still deserves to be investigated.

Here, we demonstrate the wave-domain heat transfer mechanism under steady high heat fluxes again in graphene. And by systematically analyzing the influences of the bond length, heat flux, boundary conditions, system length and simulation parameters on the frequency of the mechanical wave using a non-equilibrium molecular dynamics (NEMD) method, we find two triggering factors of this anomalous heat conduction phenomenon, that is, the heat flux and the strain, and further we discuss the underlying mechanism of the wave-domain heat conduction.

2. Simulation detail

In this work, we systematically investigate the non-Fourier heat conduction of the zigzag-edged graphene sheet under steady state in models with Brenner potential [27], by using NEMD method [10, 14,23,28,29]. In the MD simulations, periodic boundary conditions are used along the length direction, and as for the width direction,

* Corresponding author. Fax: +86 10 6279 4531.

E-mail address: caoby@tsinghua.edu.cn (B.-Y. Cao).

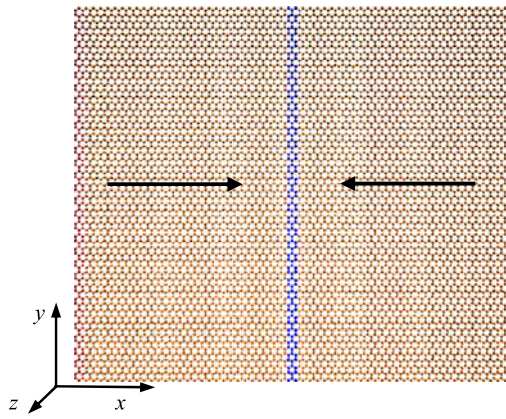


Fig. 1. Schematic of simulation system including a high-temperature slab (red) and a low-temperature slab (blue). (Color online.)

we performed free and periodic boundary conditions respectively and no qualitative changes are found on the conclusions.

As illustrated in Fig. 1, the heat current is from the high-temperature slab (the red atoms on the side) to the low-temperature slab (the blue atoms in the middle), which is imposed by using the velocity exchange method developed by Müller [30] and calculated from Eq. (1):

$$J = \frac{\sum_{\text{transfers}} \frac{m}{2} (v_h^2 - v_c^2)}{t}, \quad (1)$$

in which m is the atomic mass of carbon, v_h is the velocity of the hottest atom in the low-temperature slab, v_c is the velocity of the coldest atom in the high-temperature slab, t is the statistical time. Total energy and momentum of the system are conserved during the velocity-exchange, while the system temperature is kept at 300 K with the Nosé–Hoover thermostat [31]. The atomic motion is integrated by the leap-frog scheme with a fixed time step of 0.5 fs. Each simulation case runs for 1 ns to reach a steady state, and then for 1.5 ns to average the temperature, heat flux, and bond-length over time. During the simulation, the system is equally divided into 50 slabs along the length direction, and the local instantaneous temperature for each slab, according to the energy equipartition theorem, is defined through the averaged kinetic energy as:

$$T_i = \frac{2}{3N_i k_B} \sum_{j=1}^{N_i} \frac{P_j^2}{2m}, \quad (2)$$

where N_i is the atom number of i -th slab, k_B is the Boltzmann constant and P_j is the momentum of the j -th atom.

3. Results and discussion

Imposing a small heat flux into graphene, heat is transported following Fourier's heat conduction law and a typical configuration is observed, as shown in Fig. 2. We know that the stability of two-dimensional (2D) materials has not been very clear yet [32–34]. From our simulations, the first thing to note is that the spatial distribution of carbon atoms is not perfectly two-dimensional. Ripples spontaneously appear under low heat fluxes. They look like randomly distributed and don't disappear with time, which is consistent with theoretical researches [35]. Thus, it is demonstrated that the graphene is not a strictly 2D crystal, and its existence doesn't contradict the argument that strictly 2D crystals are thermodynamically unstable and could not exist in a free state. Although 2D graphene embedded in a three-dimensional space has a tendency to be crumpled, the ripples are still suppressed by anharmonic coupling between bending and stretching modes, making graphene a quasi-2D structure.

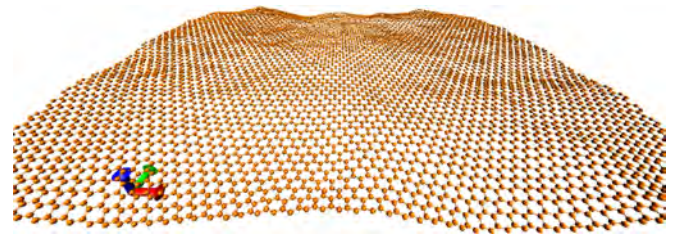


Fig. 2. Snapshot of ripples in simulation system.

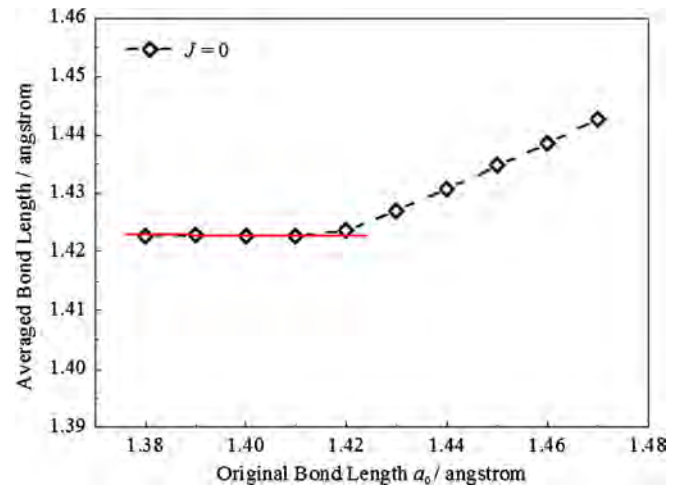


Fig. 3. Averaged bond length \bar{a} of systems with a heat flux $J = 0$ versus original bond length a_0 . (Color online.)

Additionally, ripples also introduce strain into the simulation systems. Fig. 3 shows the averaged bond length \bar{a} of systems with a heat flux $J = 0$, calculated after reaching a steady state, as a function of the original bond length a_0 , set before simulation. It can be seen from the red line in Fig. 3, as the original bond length increases from 1.38 Å to 1.41 Å, the averaged bond length stays the same and is always larger than the original one, suggesting that systems with bond length equal to or smaller than 1.41 Å are initially compressed. But because no restrictions are on the out-of-plane direction in graphene due to its quasi-2D structure, the graphene sheet can only be crumpled while its bond length cannot be decreased. However, with larger original bond length, the averaged bond length increases gradually, indicating that the systems with the original bond length of 1.42~1.47 Å are stretched to different degree at the steady state. Some researches give the unstrained bond length of graphene is 1.42 Å [36–38], which is in accordance with our conclusion that no stress is in the systems with the bond length smaller than 1.42 Å, but because of the existence of the ripples mentioned before, the systems with the original bond length equal to 1.42 Å are also stretched in our simulations.

In our simulations, under a small heat flux, ripples spontaneously appear and heat is transported by phonons, i.e., the lattice vibrations, following Fourier's heat conduction law, in both strained and unstrained graphene. But when the heat flux exceeds a critical value, a mechanical wave may be observed, which is quite different from ripples. It provides an additional channel for the non-Fourier heat conduction and enables graphene more conductive, which we will mainly focus on in this paper. For example, we impose a heat flux of 2713 GW/m², high enough to excite the mechanical wave, into the pristine graphene. Then we calculate the temperature profiles and gave some images of the real system at different time, presented in Figs. 4(a) and 4(b).

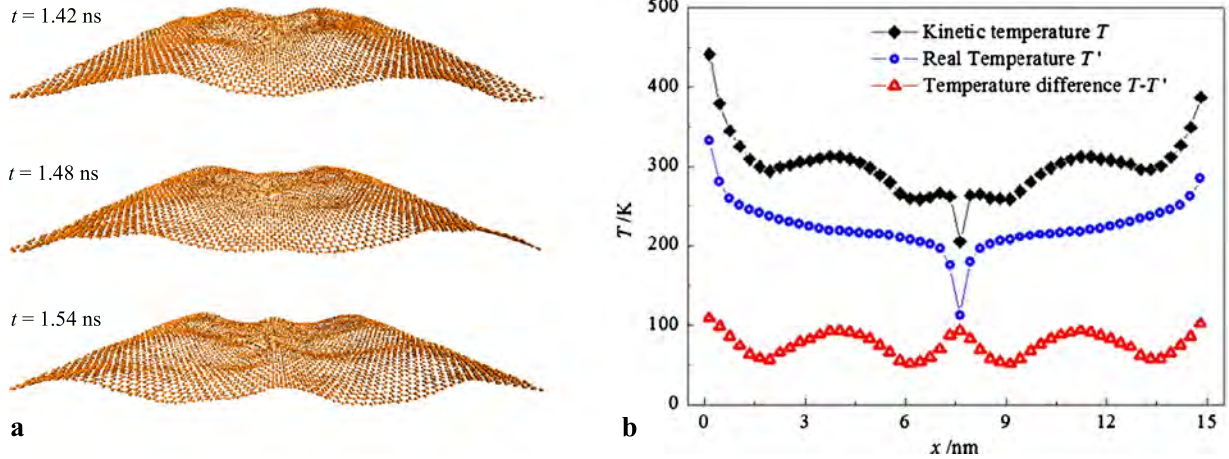


Fig. 4. (a) Typical configurations of graphene under high heat flux at different time. (b) Profiles of kinetic temperature T , real temperature T' and temperature difference $T - T'$. (Color online.)

We can see from Fig. 4(a) that the graphene sheet vibrates significantly, especially in the out-of-plane direction. The fluctuations are distributed regularly and vary with time. They look like a wave and quite different from ripples. Its counterpart is a wave-like temperature profile shown by the black squares in Fig. 4(b). Typically, if there is macroscopic momentum in the system, the kinetic temperature defined by Eq. (2) can only represent the total energy but not the internal thermal energy of random motions [39]. So, the wave-like kinetic temperature profile only means a wave-like total energy profile here. Thus, to further analyze the heat conduction, we decompose the total kinetic temperature T into a real temperature T' defined by excluding the local momentum in each slab as Eq. (3), which presents the internal thermal energy, and a temperature difference between T and T' , which presents the external mechanical energy.

$$T'(x) = \frac{m}{3Nk_B} \sum_{i=1}^N \left(v_i - \frac{P_i}{m} \right)^2. \quad (3)$$

The results are shown in Fig. 4(b). As shown, the distribution of the real temperature between the high and low thermostat slabs is linear, in accordance with Fourier's heat conduction law. And the distribution of the remaining external energy is sinusoidal, indicating that a mechanical wave is excited by the high heat flux of 2713 GW/m^2 . This phenomenon is consistent with that in CNTs [24]. But the difference is, in CNT, waves are only found in the cases with the heat sources at center but not with a heat current in an opposite direction like the case shown in Fig. 1.

Time dependent x -, y - and z -translational displacements of atoms under a heat flux of 3616 GW/m^2 are shown in Figs. 5(a)–(c). Consistent with Fig. 4(a), atoms vibrate periodically, especially in z direction, and they are always around their equilibrium positions on all three degrees of freedoms. The vibration amplitude and frequency are calculated by a Fourier transform and shown in Fig. 5(d). As shown, firstly, for z direction, the main frequency of the mechanical wave is 0.34 THz . And its corresponding amplitude is 3.30 \AA , much larger than that of ripples or random vibrations of atoms under low heat flux. Secondly, for x direction, the amplitude is 0.46 \AA . The main frequency is 0.68 THz , which is twice that in z direction, and they both go far below the random vibration frequency by 2 orders of magnitude, so it is called low-frequency wave [24,25]. Finally, for y direction, several peaks are around 0.60 THz . But the maximum amplitude is only 0.10 \AA , about 7% of the carbon–carbon bond length. Therefore, the component in y direction can be ignored and the low-frequency mechanical wave excited by the high heat flux can be decomposed into one trans-

verse and one longitudinal wave. They appear simultaneously in our simulations and the frequency of the wave in z direction is always half of that in x direction.

The percentage of the energy transported by this mechanical wave and corresponding pristine thermal conductivity of graphene can be calculated according to the following formulas, respectively.

$$R = \frac{P_{\text{wave}}}{P_{\text{total}}} = \frac{2\pi^2 \mu f^2 A^2 v_g}{J A_c}, \quad (4a)$$

$$k = \frac{J A_c - 2\pi^2 \mu f^2 A^2 v_g}{-A_c \nabla T}. \quad (4b)$$

Here, P_{wave} is the thermal power of the mechanical wave, μ is the mass of the graphene per unit length, f and A are the wave frequency and amplitude, respectively, A_c is the cross-sectional area, v_g is the wave speed obtained through tracking crest location [23] and ∇T is calculated by fitting the linear real temperature profile. The results versus the heat flux are shown in Fig. 6. In Fig. 6(a), at low heat fluxes, no mechanical waves are excited in the system and heat is totally transported by the normal Fourier heat conduction, so the thermal conductivity obtained under low heat flux is the pristine thermal conductivity of graphene. As the heat flux exceeds a critical value, the percentage of the energy transported by this mechanical wave increases with the increasing heat flux, which is up to 90% in our simulations and approaching to the limit of 100%. Meanwhile the thermal conductivities under high heat fluxes shown in Fig. 6(b) are almost equal to the pristine value under low heat fluxes, and they always stabilize around their averaged value shown by the dotted line no matter whether the mechanical wave is excited or not. In a word, the mechanical wave provides an additional channel to conduct the high heat flux, which is independent from the Fourier heat conduction and render graphene significantly more energy conductive without changing its pristine thermal conductivity. In addition, we study the length dependence of the wave-domain heat conduction mechanism, shown in Fig. 6. Interestingly, the ratio of wave-transported energy is found to decrease with increasing system length under same heat flux, while the thermal conductivity and critical heat flux are increased. This is consistent to the conclusion from Zhang et al. [24] that the low-frequency mechanical wave is more difficult to be excited in longer systems which have higher thermal conductivity and can transport energy more effectively than shorter systems.

Also, we calculate the wave amplitude by the Fourier transform and the thermal power of the mechanical wave according

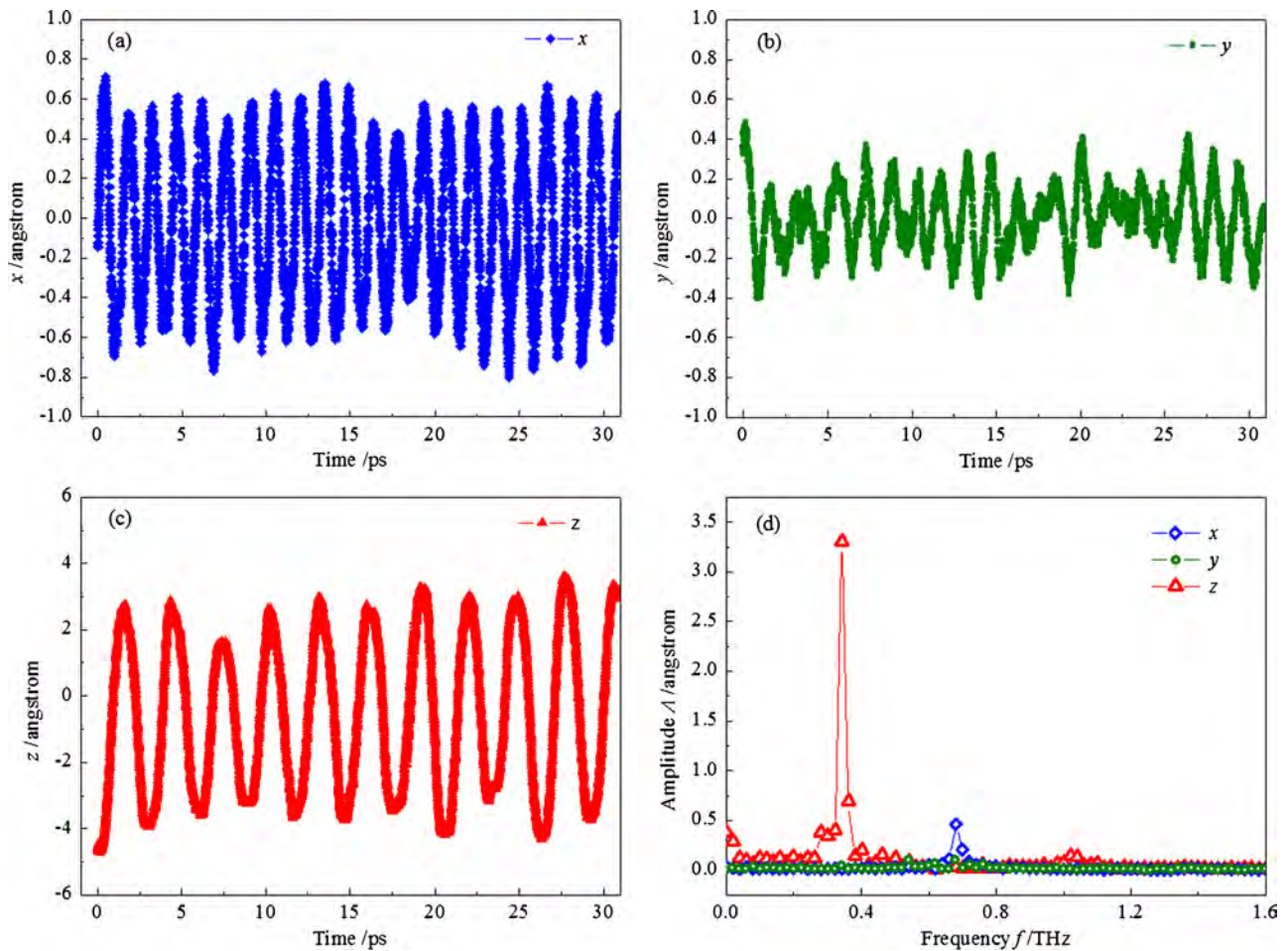


Fig. 5. (a)–(c) Translational displacement of atom under heat flux of 3616 GW/m^2 in x , y and z directions versus time. (d) Corresponding vibration amplitude versus frequency. (Color online.)

to Eq. (4a), at different locations between two thermostat regions. As shown in Table 1, the energy transported by the mechanical wave decreases slowly from the high-temperature region to the low-temperature region, indicating that a portion of mechanical energy is dissipated. But we can also find that the amount of the dissipation is very small. In addition, we have known from Fig. 4(b) that the distribution of the real temperature between the high and low thermostat slabs is almost linear, indicating that no or negligible additional thermal energy is injected or removed. So we can deduce from these two aspects that there is a small amount of damping dissipation during the wave transport.

The main frequency of the mechanical wave component in the out-of-plane direction with respect to the heat flux and the original bond length, ranging from 1.39 \AA to 1.46 \AA , are summarized in Fig. 7, where frequency of 0 means no mechanical waves and higher frequency means more mechanical energy transported since the energy of the mechanical wave is proportional to the square of its frequency according to Eq. (4a). As shown, at all low heat fluxes, no mechanical waves are excited and heat is totally transported by the Fourier heat conduction. And as the heat flux exceeds a critical value, things are same in the cases with original bond length less than 1.42 \AA , while in the cases equal to or larger than 1.42 \AA , the mechanical wave is excited and its frequency increases with the increasing heat flux or increasing original bond length, namely, the tensile stress, with other conditions unchanged, respectively. Thus, we can conclude that two necessary factors to trigger the mechanical wave are steady high heat flux and tensile stress. What's more, as shown in Fig. 7, the critical heat flux of graphene sheet

is about 2200 GW/m^2 , which is much larger than those for hybrid graphene/silicene monolayer ($\sim 42 \text{ GW/m}^2$) [26], the 400-nm-long (5, 5) carbon nanotube ($\sim 241 \text{ GW/m}^2$) [24] and the 21.7-nm-long graphene nanoribbon ($\sim 400 \text{ GW/m}^2$) [25]. And except for the case with original bond length $a_0 = 1.42 \text{ \AA}$, the critical value of the heat flux increases slightly with the bond length increasing, indicating that the critical heat flux of graphene sheet is proportional to the strain.

In NEMD simulations, the heat flux imposed by exchanging atom velocities can be regarded as multiple heat pulses, specifically, which is determined by both velocity exchange intervals, i.e., the pulse frequency, and exchange atom numbers at each time, i.e., the pulse energy. The main wave frequencies of cases with nine sets of different pulse frequency and pulse energy are shown in Fig. 8. Different from the effect of the heat flux shown in Fig. 7, whether the mechanical wave is excited or not and the frequency of the mechanical wave have no obvious relation with the above two factors, which indicates that the high-frequency or high-energy pulses are not the root reasons of triggering the mechanical waves, also that this anomalous phenomenon is not the artifact of the velocity-exchange method.

Heat conduction in graphene is a typical non-equilibrium process. With a lower heat flux, the non-equilibrium system satisfies the local thermodynamic equilibrium assumption. The force has a linear correlation with the flow, which is the Fourier heat conduction law. But when the heat flux exceeds the critical value, a new order state far from thermodynamic equilibrium at macro level, that is, dissipative structure [40], is formed. The term dis-

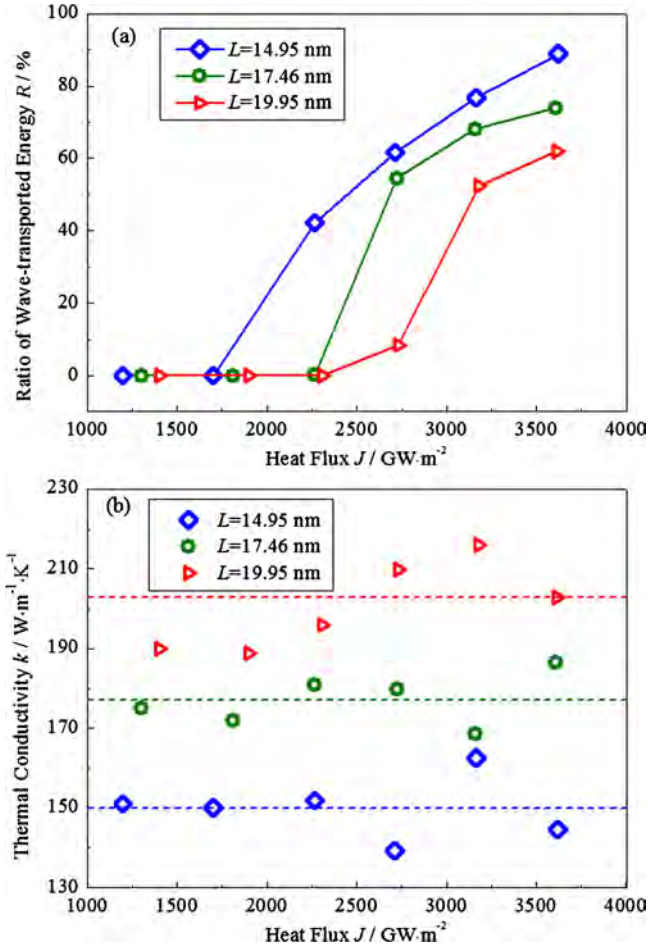


Fig. 6. (a) Ratio of energy transported by mechanical wave and (b) pristine thermal conductivity of graphene. (Color online.)

Table 1

Amplitude and thermal power of mechanical wave at different locations under heat flux of $3616\text{ GW}/\text{m}^2$.

| Location (x, y)/nm | Amplitude $A/\text{\AA}$ | Thermal power of mechanical wave P_{wave}/W |
|---------------------------|-----------------------------|--|
| (11.0, 1.9) | 2.9 | $5.3\text{E}-06$ |
| (11.5, 1.9) | 3.0 | $5.5\text{E}-06$ |
| (12.0, 1.9) | 3.1 | $5.6\text{E}-06$ |
| (12.5, 1.9) | 3.3 | $5.8\text{E}-06$ |

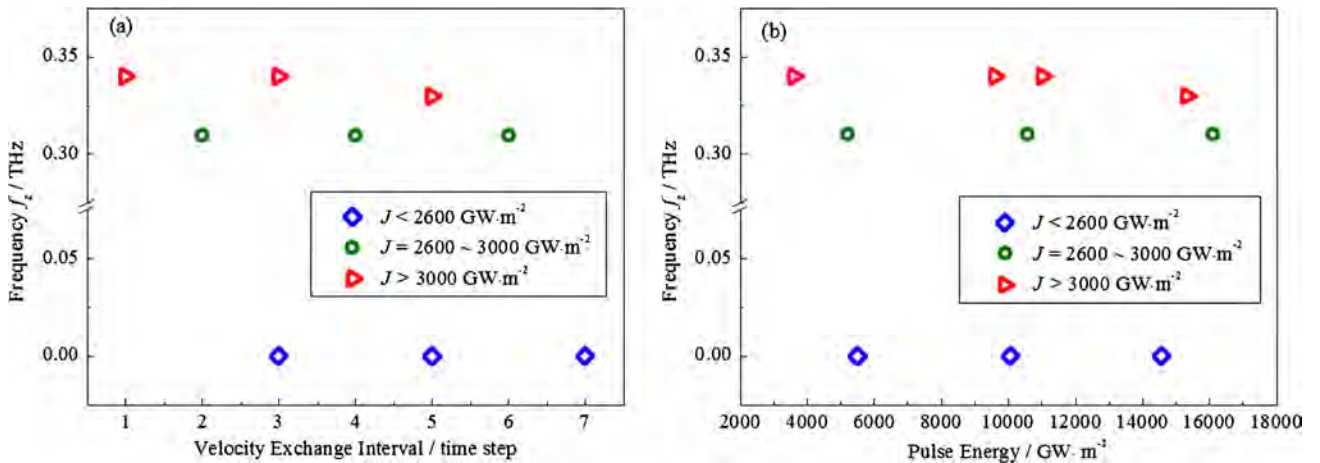


Fig. 8. Main frequency of mechanical wave in z direction versus the simulation parameters: (a) velocity exchange interval (i.e. pulse frequency) and (b) pulse energy (i.e. exchange atom number). (Color online.)

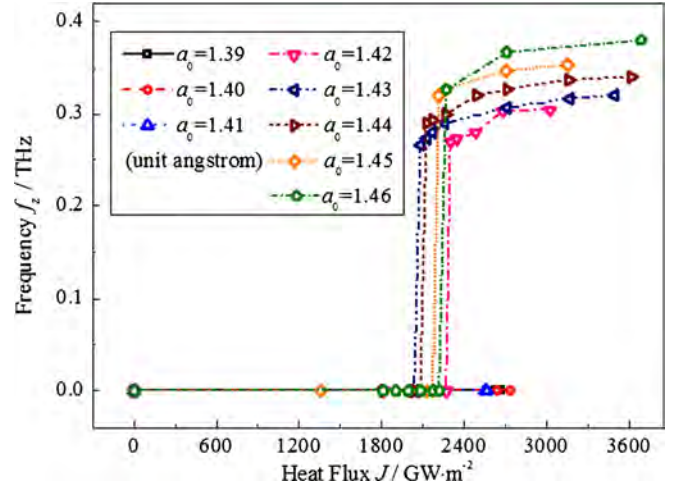


Fig. 7. Main frequency of the mechanical wave in z direction with respect to heat flux and original bond length. (Color online.)

sipative structure is coined by Ilya Prigogine [41] to distinguish from “equilibrium” structures such as the flat 2D crystal structure of graphene. And it means a new space–time structure of dynamical system in far-from-equilibrium situations, where stability is not the only result of general laws of physics and any fluctuations may no longer be damped but be amplified gradually with time and invade the whole system until reach a reproducible steady state. The dissipative structure is common in everyday life, such as turbulent flow and hurricane. And in our simulations, it is ripple in unstrained graphene and is mechanical wave in strained graphene because the development of ripples is restrained by tensile stress. As a result, in strained graphene, the force has a complicated non-linear relationship with the flow, which is the non-Fourier heat conduction we discussed in this paper, and compared with the Fourier heat conduction, the mechanical wave enables more efficient heat transport in graphene, which makes graphene possible

for thermoelectrics and more thermal management applications under high heat fluxes.

4. Conclusion

In this paper, we systematically investigate the non-Fourier heat conduction in graphene under steady high heat fluxes using NEMD method, and a mechanical wave, quite different from the ripples, and corresponding wave-like temperature profiles are observed. Main conclusions in terms of the wave-domain thermal transport in graphene are as follows:

- (1) Two triggering factors of this anomalous wave-domain energy transport phenomenon are: the high steady heat flux and the tensile stress. A mechanical wave can only be excited by high heat fluxes in strained graphene.
- (2) This mechanical wave provides an additional channel of heat transport independent from the Fourier heat conduction and enables graphene more conductive without changing its pristine thermal conductivity. Its main frequency is smaller than that of the random vibrations by about two orders and increases with the increasing heat flux or increasing original bond length, respectively. What's more, the energy transported by the mechanical wave increases with the increasing heat flux.
- (3) This anomalous phenomenon is not arising from the high-energy or high-frequency pulses and also not artifacts induced by the velocity-exchange method. It is a dissipative structure, a new order state far from thermodynamic equilibrium, and its corresponding temperature gradient has a complicated non-linear relationship with the heat flux, which enables more efficient heat transport in graphene. A constructive equation relating the heat flux to the temperature gradient is highly desired for further studies.

Abbreviations

2D: two-dimensional; CNT: carbon nanotube; NEMD: non-equilibrium molecular dynamics.

Acknowledgement

This work was supported by the National Natural Science Foundation of China (Grant Nos. 51322603, 51136001, 51356001), Science Fund for Creative Research Groups (No. 51321002), the Program for New Century Excellent Talents in University, Tsinghua University Initiative Scientific Research Program, and the Tsinghua National Laboratory for Information Science and Technology of China.

References

- [1] S. Ghosh, I. Calizo, D. Teweldebrhan, et al., Extremely high thermal conductivity of graphene: prospects for thermal management applications in nanoelectronic circuits, *Appl. Phys. Lett.* 92 (15) (2008) 151911.
- [2] A.K. Geim, P. Kim, Carbon wonderland, *Sci. Am.* 298 (4) (2008) 90.
- [3] E. Pop, V. Varshney, A.K. Roy, Thermal properties of graphene: fundamentals and applications, *Mater. Res. Soc. Bull.* 37 (12) (2012) 1273.
- [4] Z. Yan, D.L. Nika, A.A. Balandin, Thermal properties of graphene and few-layer graphene: applications in electronics, *IET Circuits Devices Syst.* 9 (1) (2015) 4.
- [5] A.A. Balandin, S. Ghosh, W. Bao, et al., Superior thermal conductivity of single-layer graphene, *Nano Lett.* 8 (3) (2008) 902.
- [6] J. Hu, X. Ruan, Y.P. Chen, Thermal conductivity and thermal rectification in graphene nanoribbons: a molecular dynamics study, *Nano Lett.* 9 (7) (2009) 2730.
- [7] J.H. Seol, I. Jo, A.L. Moore, et al., Two-dimensional phonon transport in supported graphene, *Science* 328 (5975) (2010) 213.
- [8] A.A. Balandin, Thermal properties of graphene and nanostructured carbon materials, *Nat. Mater.* 10 (8) (2011) 569–581.
- [9] Y. Xu, Z. Li, W. Duan, Thermal and thermoelectric properties of graphene, *Small* 10 (11) (2014) 2182.
- [10] Z.Q. Ye, B.Y. Cao, W.J. Yao, et al., Spectral phonon thermal properties in graphene nanoribbons, *Carbon* 93 (2015) 915.
- [11] J.W. Jiang, B.S. Wang, J.S. Wang, First principle study of the thermal conductance in graphene nanoribbon with vacancy and substitutional silicon defects, *Appl. Phys. Lett.* 98 (11) (2011) 113114.
- [12] P.H. Chang, M.S. Bahrany, N. Nagaosa, et al., Giant thermoelectric effect in graphene-based topological insulators with heavy adatoms and nanopores, *Nano Lett.* 14 (7) (2014) 3779.
- [13] T. Feng, X. Ruan, Z. Ye, et al., Spectral phonon mean free path and thermal conductivity accumulation in defected graphene: the effects of defect type and concentration, *Phys. Rev. B* 91 (22) (2015) 224301.
- [14] B.Y. Cao, W.J. Yao, Z.Q. Ye, Networked nanoconstrictions: an effective route to tuning the thermal transport properties of graphene, *Carbon* 96 (2016) 711.
- [15] D.W. Boukhvalov, M.I. Katsnelson, Chemical functionalization of graphene, *J. Phys. Condens. Matter* 21 (34) (2009) 344205.
- [16] V. Georgakilas, M. Otyepka, A.B. Bourlinos, et al., Functionalization of graphene: covalent and non-covalent approaches, derivatives and applications, *Chem. Rev.* 112 (11) (2012) 6156.
- [17] F. Ma, H.B. Zheng, Y.J. Sun, et al., Strain effect on lattice vibration, heat capacity, and thermal conductivity of graphene, *Appl. Phys. Lett.* 101 (11) (2012) 111904.
- [18] L. Lindsay, W. Li, J. Carrete, et al., Phonon thermal transport in strained and unstrained graphene from first principles, *Phys. Rev. B* 89 (15) (2014) 155426.
- [19] H. Sevinçli, C. Sevik, T. Çağın, et al., A bottom-up route to enhance thermoelectric figures of merit in graphene nanoribbons, *Sci. Rep.* 3 (2013).
- [20] L. Yang, J. Chen, N. Yang, et al., Significant reduction of graphene thermal conductivity by phononic crystal structure, arXiv preprint, arXiv:1407.5885, 2014.
- [21] M.A. Osman, D. Srivastava, Molecular dynamics simulation of heat pulse propagation in single-wall carbon nanotubes, *Phys. Rev. B* 72 (12) (2005) 125413.
- [22] J. Shiomoto, S. Maruyama, Non-Fourier heat conduction in a single-walled carbon nanotube: classical molecular dynamics simulations, *Phys. Rev. B* 73 (2006) 205420.
- [23] W.J. Yao, B.Y. Cao, Thermal wave propagation in graphene studied by molecular dynamics simulations, *Chin. Sci. Bull.* 59 (27) (2014) 3495.
- [24] X. Zhang, M. Hu, D. Poulidakos, A low-frequency wave motion mechanism enables efficient energy transport in carbon nanotubes at high heat fluxes, *Nano Lett.* 12 (7) (2012) 3410.
- [25] K. Zheng, L. Wang, S. Bai, et al., An anomalous wave-like kinetic energy transport in graphene nanoribbons at high heat flux, *Physica B, Condens. Matter* 434 (2014) 64.
- [26] B. Liu, J.A. Baimova, C.D. Reddy, et al., Interface thermal conductance and rectification in hybrid graphene/silicene monolayer, *Carbon* 79 (2014) 236.
- [27] D.W. Brenner, Empirical potential for hydrocarbons for use in simulating the chemical vapor deposition of diamond films, *Phys. Rev. B* 42 (15) (1990) 9458.
- [28] B.Y. Cao, Y.W. Li, A uniform source-and-sink scheme for calculating thermal conductivity by nonequilibrium molecular dynamics, *J. Chem. Phys.* 133 (2) (2010) 024106.
- [29] G.J. Hu, B.Y. Cao, Thermal resistance between crossed carbon nanotubes: molecular dynamics simulations and analytical modeling, *J. Appl. Phys.* 114 (22) (2013) 224308.
- [30] F. Müller-Plathe, A simple nonequilibrium molecular dynamics method for calculating the thermal conductivity, *J. Chem. Phys.* 106 (14) (1997) 6082.
- [31] W.G. Hoover, Canonical dynamics: equilibrium phase-space distributions, *Phys. Rev. A* 31 (3) (1985) 1695.
- [32] R. Peierls, Quelques propriétés typiques des corps solides, *Ann. Inst. Henri Poincaré* 5 (3) (1935) 177.
- [33] L. Landau, D. Zur, Theorie der phasenumwandlungen II, *Phys. Z. Sowjetunion* 11 (1937) 26.
- [34] M.H. Gass, U. Bangert, A.L. Bleloch, et al., Free-standing graphene at atomic resolution, *Nat. Nanotechnol.* 3 (11) (2008) 676.
- [35] A. Fasolino, J.H. Los, M.I. Katsnelson, Intrinsic ripples in graphene, *Nat. Mater.* 6 (11) (2007) 858.
- [36] R. Saito, G. Dresselhaus, M.S. Dresselhaus, *Physical Properties of Carbon Nanotubes*, Imperial College Press, London, 1998.
- [37] D.L. Nika, E.P. Pokatilov, A.S. Askerov, et al., Phonon thermal conduction in graphene: role of Umklapp and edge roughness scattering, *Phys. Rev. B* 79 (15) (2009) 155413.
- [38] J.W. Jiang, J.S. Wang, B. Li, Thermal conductance of graphene and dimerite, *Phys. Rev. B* 79 (20) (2009) 205418.
- [39] Y. Dong, B.Y. Cao, Z.Y. Guo, Temperature in nonequilibrium states and non-Fourier heat conduction, *Phys. Rev. E* 87 (3) (2013) 032150.
- [40] R.S. Li, *Non-Equilibrium Thermodynamics and Dissipative Structure*, 1986 (in Chinese).
- [41] D. Kondepudi, I. Prigogine, *Modern Thermodynamics: From Heat Engines to Dissipative Structures*, John Wiley & Sons, 2014.